Epitaxial growth of Fe3Si/CaF2/Fe3Si magnetic tunnel junction structures on CaF2/Si(111) by molecular beam epitaxy

著者	Kobayashi Ken'ichi, Suemasu Takashi, Kuwano Noriyuki, Hara Daisuke, Akinaga Hiroyuki
journal or publication title	Thin solid films
volume	515
number	22
page range	8254-8258
year	2007-08
権利	(C) 2007 Elsevier B.V
URL	http://hdl.handle.net/2241/97880

doi: 10.1016/j.tsf.2007.02.057

Epitaxial growth of $Fe_3Si/CaF_2/Fe_3Si$ magnetic tunnel junction structures on $CaF_2/Si(111)$ by molecular beam epitaxy

Ken'ichi Kobayashi[a], Takashi Suemasu[a], Noriyuki Kuwano[b], Daisuke Hara[b] and Hiroyuki Akinaga[c]

[a]*Institute of Applied Physics, University of Tsukuba, Tsukuba, Ibaraki 305-8573, Japan*

[b]*Department of Applied Science for Electronics and Materials, Kyushu University, 6-1 Kasuga, Fukuoka 816-8580, Japan*

[c]*Nanoelectronics Research Institute, National Institute of Advanced Industrial Science and Technology, Tsukuba, Ibaraki 305-8568, Japan*

The Fe_3Si(24 nm)/CaF_2(2 nm)/Fe_3Si(12 nm) magnetic tunnel junction (MTJ) structures were grown epitaxially on $CaF_2/Si(111)$ by molecular beam epitaxy (MBE). The 12-nm-thick Fe_3Si underlayer was grown epitaxially on $CaF_2/Si(111)$ at approximately 400°C; however, the surface of the Fe_3Si film was very rough, and thus a lot of pinholes are considered to exist in the 2-nm-thick CaF_2 barrier layer. The average roughness (Ra) of the CaF_2 barrier layer was 7.8 nm. This problem was overcome by low temperature deposition of Fe and Si at 80°C on $CaF_2/Si(111)$, followed by

annealing at 250°C for 30 min to form the Fe_3Si layer. The Ra roughness was significantly reduced down to approximately 0.26 nm. A hysteresis loop with coercive field H_c of approximately 25 Oe was obtained in the magnetic field dependence of Kerr rotation at room temperature (RT).

KEYWORDS: ferromagnetism, Fe_3Si, CaF_2, Si

Corresponding author: Prof. T. Suemasu, Institute of Applied Physics, University of Tsukuba, Tsukuba, Ibaraki 305-8573, Japan.

TEL(FAX): +81-29-853-5111, Email: suemasu@bk.tsukuba.ac.jp

1. Introduction

In recent years, magnetic materials have been developed to be used in magnetic tunnel junctions (MTJs). They consist of two ferromagnetic electrodes separated by a barrier layer, and show the tunnel magnetoresistance (TMR) effect [1,2]. This phenomenon has been applied to magnetoresistive random access memory (MRAM). Since an MRAM has been proposed as a universal memory [3], in which not only high-speed operation in a static random-access memory (SRAM) but also high integrity in a dynamic random-access memory (DRAM) can be expected. In order to achieve Gb-scale MRAM, TMR ratios exceeding 150% and higher output voltages (>190 mV) are required [4]. However, the TMR ratio of current MTJs with an amorphous barrier layer is approaching its theoretical limit. One way to overcome these difficulties is to use fully epitaxial MTJs together with highly spin–polarized ferromagnetic electrodes. We think that ferromagnetic Fe_3Si is a good candidate for such a material. Fe_3Si is ferromagnetic up to 530-570°C [5-7], and it possesses two distinct Fe sites with magnetic moments μ_{Fe}^{I}=2.2 μ_B/atom and μ_{Fe}^{II}=1.35 μ_B/atom, where μ_B is the Bohr magneton. Thus, Fe_3Si can be regarded as a Heusler alloy $Fe^{II}_2Fe^{I}Si$, (DO_3 type) [8], and therefore a candidate for being half-metallic [9]. Fe_3Si has a lattice parameter of 0.564 nm, which is nearly lattice-matched to Si. Very recently,

the epitaxial growth of Fe_3Si on Si(111) was reported [10]. However, it is difficult to prevent the formation of interfacial compounds like FeSi due to the diffusion of Si atoms from the substrate into the grown films [11], which is unfavorable for large TMR ratios. To avoid this problem, we inserted CaF_2 layers between Fe_3Si and Si substrates. CaF_2 is known to grow epitaxially on Si(111) substrates at temperatures higher than 600°C [12-14]. We have realized the epitaxial growth of Fe_3Si on CaF_2/Si(111) by molecular beam epitaxy (MBE) [11,15].

The purpose of this investigation was to form $Fe_3Si/CaF_2/Fe_3Si$ TMR structures epitaxially on CaF_2/Si(111) by MBE. Surface roughness and magnetic properties of the grown layers were also investigated.

2. Experimental

An ion-pumped MBE system equipped with electron-beam evaporation sources for Fe and Si was used. CaF_2 was evaporated by a high-temperature Knudsen cell. The Fe_3Si(24 nm)/CaF_2(2 nm)/Fe_3Si(12 nm) TMR structures were epitaxially grown on CaF_2/Si(111) by MBE as follows: first, a 50-nm-thick Si buffer layer was grown at 450ºC on Si(111) substrates. Then, wafers were annealed at 1000ºC for 30 min to improve the crystal quality. Next, 8-nm-thick CaF_2 was grown epitaxially on Si(111) at

600°C. Then, Si and Fe were co-evaporated at 400°C to form a 12-nm-thick Fe_3Si first layer, followed by a 2-nm-thick CaF_2 barrier layer grown at 600°C. Finally, a 24-nm-thick Fe_3Si 2nd layer was grown in the same manner. This sample is denoted as sample A. For comparison, the $CaF_2/Fe_3Si/CaF_2$ structure was grown at a low temperature as follows: after the growth of a 50-nm-thick Si buffer layer, 8-nm-thick CaF_2 was grown epitaxially on Si(111) at 600°C. Then, Si and Fe were co-evaporated at a low temperature of 80°C, and then annealed at 250°C for 30 min to form 20-nm-thick Fe_3Si. Finally, 2-nm-thick CaF_2 was grown at 280°C. This sample is denoted as sample B. The deposition rates of Si and Fe were kept constant at 4.0 and 2.2 nm/min, respectively. They were determined using the theoretical densities of Fe and Si to satisfy stoichiometry in Fe_3Si.

The crystalline quality of the grown films was characterized by reflection high-energy electron diffraction (RHEED) and θ-2θ X-ray diffraction (XRD). RHEED patterns were observed along the [1-10] azimuth of the Si. The surface morphology was investigated using atomic force microscopy (AFM). Magneto-optical Kerr effect (MOKE) was measured to obtain the hysteresis loop of the Kerr rotation using a 632.8 nm He–Ne laser with the magnetic field up to 1500 Oe in the film plane along the [1-10] direction of Fe_3Si.

3. Results and discussion

3.1 High-temperature growth of Fe_3Si

Figure 1 shows RHEED patterns of each stage of sample A. Figure 1(a) was taken after the thermal cleaning of the substrate. Figures 1(b-e) show RHEED patterns of the 8-nm-thick CaF_2 first layer, the 12-nm-thick Fe_3Si first layer, the 2-nm-thick CaF_2 barrier layer and the 24-nm-thick Fe_3Si second layer, respectively. Streaky RHEED pattern was observed in every stage. These results indicate that the $Fe_3Si/CaF_2/Fe_3Si$ MTJ structure was epitaxially grown on CaF_2/Si(111), although small amount of FeSi was included as shown in the θ-2θ XRD pattern of Fig. 2. Since the growth temperature of the CaF_2 second layer is much higher than 400°C, it is considered to be difficult to prevent formation of FeSi as shown in our previous paper [11]. As shown in Fig. 3, a hysteresis loop was observed at RT in the magnetic field dependence of Kerr rotation. However, a step-like hysteresis loop, which exhibits the difference in coercive field H_c between the two ferromagnetic Fe_3Si layers, was not observed. This means that the two layers are ferromagnetically coupled. Figure 4 shows the 2×2-μm^2-area AFM top view and cross-sectional profile of sample A. It was found that the surface of sample A was very rough; the average roughness Ra was 7.8 nm. This roughness is attributed to the

rough surface of the Fe_3Si first layer as shown in Fig. 5. Figure 5 shows a typical example of the 2×2-μm^2-area AFM top view and cross-sectional profile taken after the growth of the 12-nm-thick Fe_3Si first layer in sample A. The Ra roughness already reaches 2.9 nm at this stage. We therefore speculate that there exist lots of pinholes in the 2-nm-thick CaF_2 barrier layer through which the two ferromagnetic Fe_3Si layers may contact. Thus, the formation of an Fe_3Si first layer with atomically flat surface is mandatory.

3.2 Low-temperature growth of Fe_3Si

In order to obtain Fe_3Si films with flat surface, we attempted low-temperature formation of Fe_3Si. Figure 6 shows RHEED patterns of each stage of sample B. Fig. 6(a) was taken after the thermal cleaning of the substrate. Fig. 6(b-e) are RHEED patterns taken after the growth of the 8-nm-thick CaF_2 first layer, after codeposition of Fe and Si at 80°C, after the subsequent annealing at 250°C for 30 min, and after the growth of the 2-nm-thick CaF_2 second layer at 280°C, respectively. As shown in Fig. 6(c), just after the codeposition of Si and Fe at 80°C, spotty RHEED pattern was observed, meaning crystalline Fe_3Si was formed even at such a low temperature. Because of the low-temperature, the surface migration of deposited Fe and Si atoms was limited, thus resulting in the spotty RHEED pattern. This spotty pattern changed into

streaky after annealing at 250°C as shown in Fig. 6(d), meaning that the rough surface was flattened. After the growth of the CaF_2 second layer at 280°C, a streaky pattern was also observed as shown in Fig. 6(e); however, it seems spotty and diffused compared to the RHEED pattern of the 2-nm-thick CaF_2 layer grown at 600°C shown in Fig. 1(d). This was caused by the low-temperature formation of the CaF_2 layer. Fig. 7 shows the 2×2-μm^2-area AFM top view and cross-sectional profile of sample B. We should note that sample B has a very smooth surface with Ra roughness=0.26 nm. The difference in the surface morphology between samples A and B is attributed to the difference in the growth temperature of the Fe_3Si first layer. A hysteresis loop is clearly seen in the magnetic field dependence of Kerr rotation as shown in Fig. 8. The coercive field H_c was approximately 25 Oe. By forming another Fe_3Si layer epitaxially on sample B, fully epitaxial MTJs together with highly spin–polarized half-metallic ferromagnetic electrodes will be obtained in the near future.

4. Conclusion

We have realized the epitaxial growth of Fe_3Si(24 nm)/CaF_2(2 nm)/Fe_3Si(12 nm) MTJ structures on CaF_2/Si(111) by MBE. However, the Ra roughness of the surface is approximately 7.8 nm. The rough surface was attributed to the surface

roughness of the Fe_3Si first layer (Ra=2.9 nm). In order to overcome this problem, Fe_3Si was formed by low-temperature codeposition of Fe and Si at 80°C, followed by 250°C annealing for 30 min. The surface morphology was greatly improved and the Ra roughness was deduced down to approximately 0.26 nm.

Acknowledgements

This work was supported in parts from the Ministry of Education, Culture, Sports, Science and Technology (MEXT) of Japan.

References

[1] T. Miyazaki, N. Tezuka, J. Magn. Magn. Mater. **139** (1995) L231.

[2] J. S. Moodera, L. R. Kinder, T. M. Wong, and R. Meservey, Phys. Rev. Lett. **74** (1995) 3273.

[3] R. E. Fontana, S. R. Hetzler, J. Appl. Phys. **99** (2006) 08N902.

[4] S. Yuasa, A. Fukushima, T. Nagahama, K. Ando, Y. Suzuki, Jpn. J. Appl. Phys., Part 2 **43** (2004) L588.

[5] A. Ôsawa, T. Murata, Nippon Kinzoku Gakkai-Shi **4** (1940) 228.

[6] M. Hong, H. S. Chen, J. Kwo, A. R. Kortan, J. P. Mannaerts, B. E. Weir, L. C. Feldman, J. Cryst. Growth **111** (1991) 984.

[7] J. Waliszewski, L. Dobrzyński, A. Malinowski, D. Satuła, K. Szymański, W. Prandl, Th. Brückel, O. Schärpf, J. Magn. Magn. Mater. **132** (1994) 349.

[8] W. A. Hines, A. H. Menotti, J. I. Budnick, T. J. Burch, T. Litrenta, V. Niculescu, K. Raj, Phys. Rev. B **13** (1976) 4060.

[9] R. A. de Groot, F. M. Mueller, P. C. Van Engen, K. H. Buschow, Phys. Rev. Lett. **50** (1983) 2024.

[10] T. Sadoh, H. Takeuchi, K. Ueda, A. Kenjo, M. Miyao, Jpn. J. Appl. Phys., Part 1 **45** (2006) 3598.

[11] T. Sunohara, K. Kobayashi, M. Umada, H. Yanagihara, E. Kita, H. Akinaga, T. Suemasu, Jpn. J. Appl. Phys., Part 2 **44** (2005) L715.

[12] H. Ishirwara, T. Asano, Appl. Phys. Lett. **40** (1982) 66.

[13] R.W. Fathauer, L.J. Schowater, Appl. Phys. Lett. **45** (1984) 519.

[14] C. A. Lucas, D. Loretto, G. C. L. Wong, Phys. Rev. B **50** (1994) 14340.

[15] K. Kobayashi, T. Sunohara, M. Umada, H. Yanagihara, E. Kita, T. Suemasu, Thin Solid Films **508** (2006) 78.

Figure captions

Figure 1 RHEED patterns of each stage of sample A. (a) was taken after the thermal cleaning of the substrate. (b), (c), (d) and (e) show RHEED patterns of the 8-nm-thick CaF_2 first layer, the 12-nm-thick Fe_3Si first layer, the 2-nm-thick CaF_2 barrier layer and the 24-nm-thick Fe_3Si second layer.

Figure 2 θ-2θ XRD pattern of sample A.

Figure 3 Magnetic field dependence of Kerr rotation obtained at RT for sample A in longitudinal geometry.

Figure 4 AFM top view and cross-sectional profile of sample A.

Figure 5 AFM top view and cross-sectional profile of the 12-nm-thick Fe_3Si first layer in sample A.

Figure 6 RHEED patterns of each stage of sample B. (a) was taken after thermal cleaning of the substrate. (b), (c), (d) and (e) are RHEED patterns taken after the growth of the 8-nm-thick CaF_2 first layer, after codeposition of Fe and Si at 80°C, after annealing at 250°C for 30min, and after the growth of the 2-nm-thick CaF_2 second layer at 280°C, respectively.

Figure 7 AFM top view and cross-sectional profile of sample B.

Figure 8 Magnetic field dependence of Kerr rotation obtained for sample B at RT.

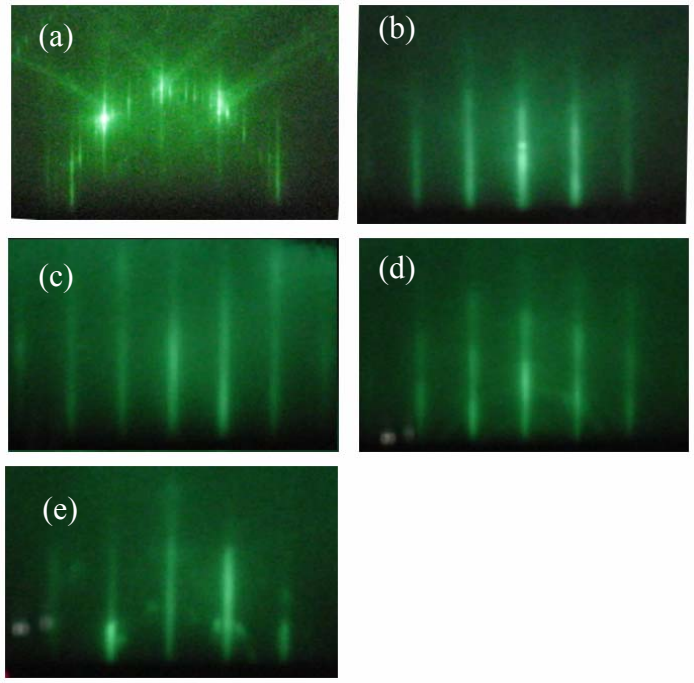

Fig. 1 Kobayashi *et al*.

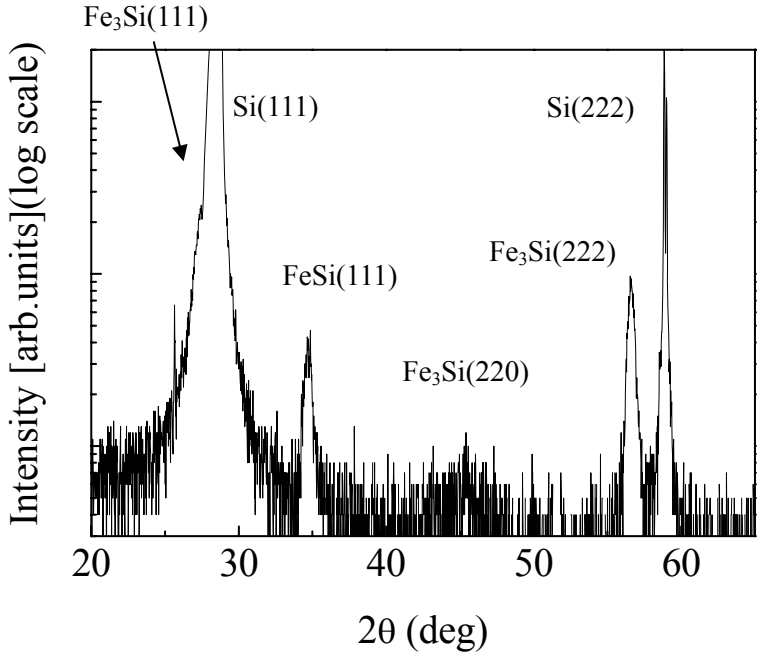

Fig. 2 Kobayashi *et al*.

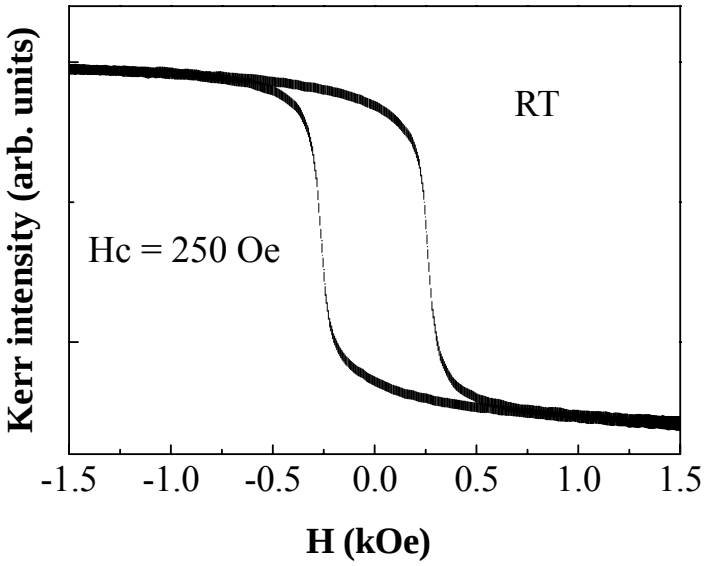

Fig. 3 Kobayashi *et al*.

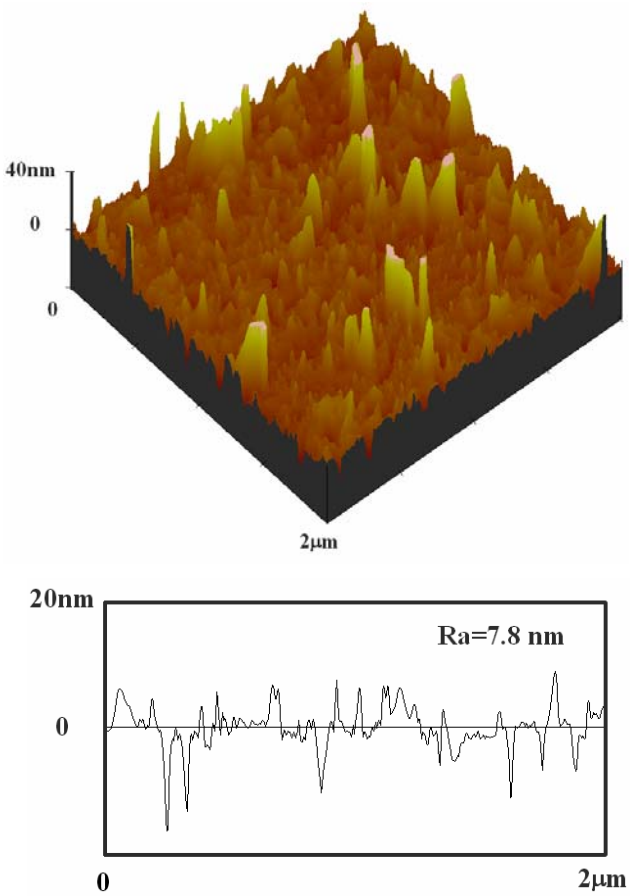

Fig. 4 Kobayashi *et al*.

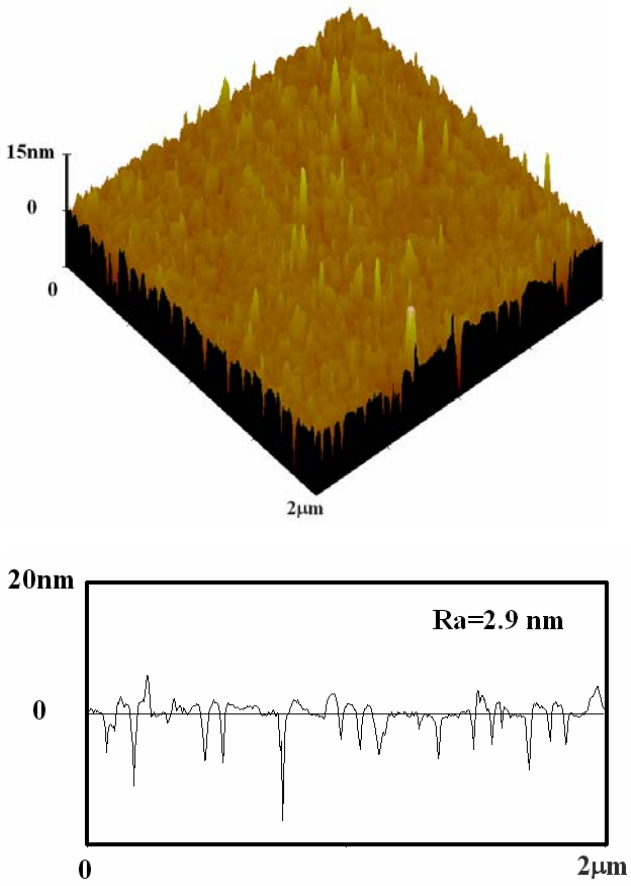

Fig. 5 Kobayashi *et al*.

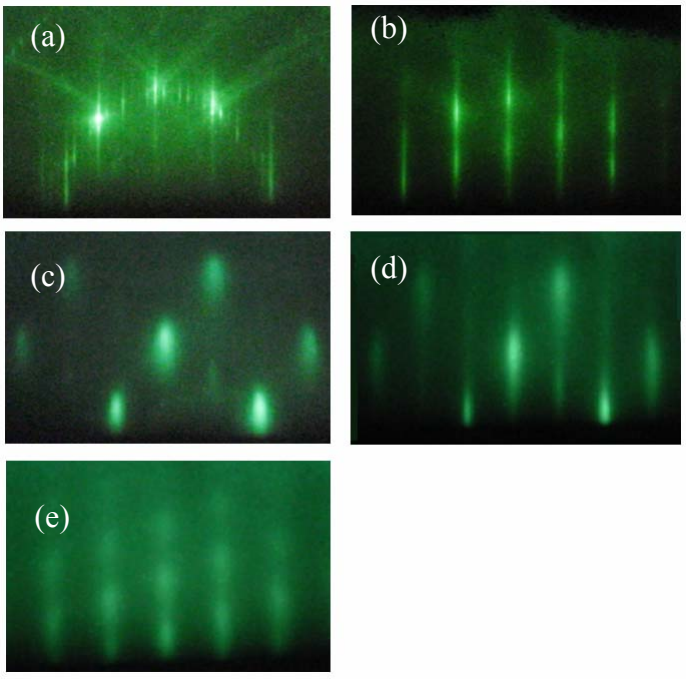

Fig. 6 Kobayashi *et al*.

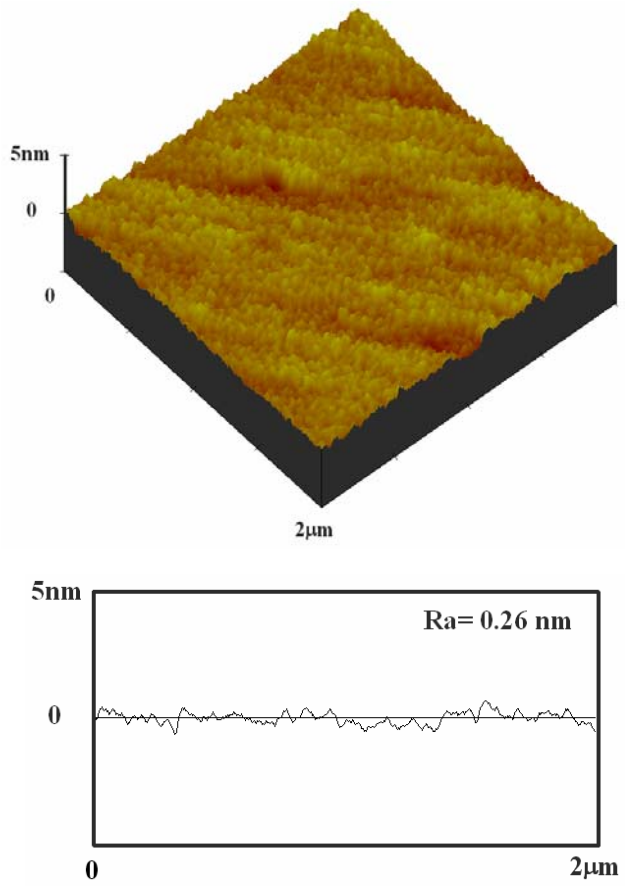

Fig. 7 Kobayashi *et al*.

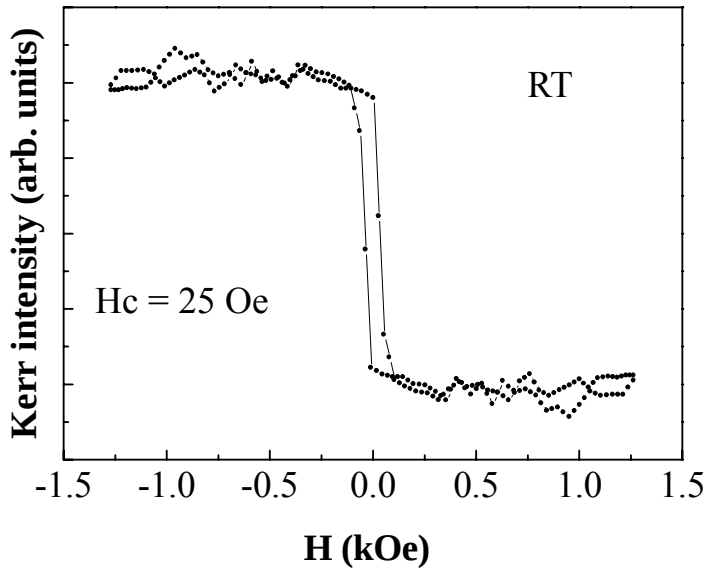

Fig. 8 Kobayashi *et al*.